Astrophys Space Sci (2020) 365:140
https://doi.org/10.1007/s10509-020-03853-y

ORIGINAL ARTICLE

Effect of suprathermal particles on EMEC instability in kappa-Maxwellian distributed space plasmas

M. Nazeer[1] · M.N.S. Qureshi[1] · H.A. Shah[2] · C. Shen[3]

Received: 18 February 2020 / Accepted: 6 August 2020 / Published online: 14 August 2020

Abstract The present study reveals the role of suprathermal particles on the destabilization of EMEC instability modelled by kappa-Maxwellian distribution and the results are compared with bi-Maxwellian results. Presence of suprathermal particles in the velocity distribution functions indicates the highly nonthermal state of plasma having large amount of free energy which is expected to enhance the kinetic instabilities. However, most of the studies on EMEC waves using bi-kappa model showed the inhibiting effect of suprathermal particles on the instability. To address this effect in kappa-Maxwellian plasmas, following Lazar et al. (2015), we proposed two variants of kappa-Maxwellian model to investigate the role of suprathermal particles on the EMEC instability in kappa-Maxwellian plasma. In kappa-Maxwellian Model-I, kappa and Maxwellian temperatures are considered to be constant while thermal velocity for kappa is taken larger than Maxwellian thermal velocity. In kappa-Maxwellian Model-II, thermal velocities for kappa and Maxwellian are considered constant while kappa temperature is taken larger than the Maxwellian temperature. We found that growth rate of EMEC waves based on the Model-I remains larger but for Model-II remains smaller than the Maxwellian growth rate. Thus in kappa-Maxwellian plasmas the Model-I truly depicted the role of suprathermal particles in enhancing the EMEC instability in contrast to bi-kappa plasmas.

✉ M.N.S. Qureshi
nouman_sarwar@yahoo.com

[1] Department of Physics, GC University, Lahore, 54000, Pakistan

[2] Department of Physics, FC College (A Charted University), Lahore, Pakistan

[3] Shenzhen Graduate School, HIT Campus, University Town of Shenzhen, Shenzhen, P.R. China

Keywords Kappa-Maxwellin distribution · EMEC waves · Effect of suprathermal particles · Kappa distribution function

1 Introduction

In many space plasmas, the suprathermal populations are the prevalent feature of solar wind, magnetospheric and auroral plasmas. Many physical scenarios such as absence of interactions and strong radiations in astrophysical plasmas, lack of collisions in solar wind and presence of parallel electric fields in auroral plasma are the robust causes for the presence of energetic/suprathermal particles in the profile of velocity distributions (Lazar et al. 2015 and references therein). The presence of such suprathermal particles are the manifestation of the deviation of plasma from thermal equilibrium. Direct observations of solar wind plasma verify this fact by providing evidence for the departure from a Maxwellian distribution and also point towards the cause of this deviation (Marsch 2006). Such nonthermal states depicted by particle velocity distributions are reflected by the presence of temperature anisotropy in the distribution and abundance of suprathermal particles reflected by the presence of high energy tails - these are common feature of space plasma environment (Gaelzer et al. 2008; Pierrard and Lazar 2010; Lazar et al. 2012). The velocity distributions possessing nonthermal features like enhanced high energy tails or flat tops are usually characterized by non-Maxwellian velocity distributions such as kappa distribution (Summers and Thorne 1991; Lazar 2012) and generalized (r, q) distribution function (Qureshi et al. 2004, 2014, 2019; Sehar et al. 2019).

Bi-Maxwellian distribution has been employed over decades to depict the temperature anisotropy in the particle velocity distributions and to describe associated waves and

instabilities in solar wind, magnetosphere, auroral regions etc. (Wu et al. 1989; Gary 1993; Treumann and Baumjohann 1997). Solar wind observations of two component velocity distribution functions showed that bi-Maxwellian distribution is the most suitable distribution to fit the low energy (core) component of the distribution which represents approximately 90 to 95% of whole population while the suprathermal (halo) part is less dense but hot enough and highly anisotropic such that it's kinetic effects cannot be ignored. It is well established that observed velocity distributions from space plasmas having enhanced suprathermal tails are well fitted via power law function rather than by an exponential function. Amongst the power law functions, kappa distribution is the most appropriate distribution as it gives the best fit to the suprathermal tail of the distribution. In many physical situations it is expected that particle distribution functions exhibit Maxwellian form due to equilibrium and isotropization in the perpendicular plane with respect to the ambient magnetic field and exhibit power law tail because of the preferential acceleration in the parallel direction. In such circumstances, a physically justified model having the advantage of mathematical tractability is the kappa-Maxwellian distribution first developed and applied to electrostatic waves by Hellberg and Mace (2002). Velocity distributions possessing excess of suprathermal population are ubiquitous in space plasmas and are often characterized by kappa-Maxwellian distribution particularly when magnetic effects become important (Hellberg et al. 2005; Nazeer et al. 2018). The kappa-Maxwellian distribution function comprises of 2-dimensional Maxwellian distribution in perpendicular plane and 1-dimensional kappa distribution in the parallel direction with respect to the magnetic field and has this been successfully employed in different studies (Mace and Hellberg 2003; Hellberg et al. 2005; Cattaert et al. 2007; Basu 2008; Sugiyama et al. 2015). The kappa-Maxwellian model is more general than bi-Maxwellian model which can be retrieved by using the limit $\kappa \to \infty$.

Generally it is expected that excess of free energy carried out by the suprathermal population may be used to enhance the growth or instability. However, in most of the studies investigating the effects of suprathermal population on the temperature anisotropy driven electromagnetic instabilities showed that the results are contrary to the expectation, i.e. the growth rates of these instabilities decrease with the increase in the presence of suprathermal particles (Xue et al. 1993, 1996; Mace 1998; Hellberg et al. 2005; Lazar and Poedts 2009; Lazar et al. 2011, 2013; Mace et al. 2011; Lazar 2012). Recently, Nazeer et al. (2018) studied electromagnetic electron cyclotron (EMEC) instability by employing kappa-Maxwellian model but the influence of enhanced suprathermal population inhibited the growth rate of the instability. In a recent paper, Lazar et al. (2015) studied the EMEC instability and clarified the effect of high energy particles by revisiting the existing bi-kappa models. They investigated two cases; case-I dealt with the models usually considered in many studies in which temperatures for Maxwellian and kappa distributions were taken constant, i.e. $T^K_{\perp,\parallel} = T^M_{\perp,\parallel}$ but modified thermal velocity was considered as kappa dependent, i.e. $\theta_{\perp,\parallel} = \sqrt{1 - \frac{3}{2\kappa}} u_{\perp,\parallel}$. Here $u_{\perp,\parallel} = \sqrt{\frac{2k_B T_{\perp,\parallel}}{m}}$, T is the temperature, $\perp$ and $\parallel$ stand for perpendicular and parallel directions w.r.t magnetic field respectively, and κ and M stand for kappa and Maxwellian distributions, respectively. Case-II dealt with the new proposed model by Lazar et al. (2015) in which kappa temperature was considered higher than the Maxwellian temperature as $T^\kappa_{\perp,\parallel} = \frac{2\kappa}{2\kappa-3} T^M_{\perp,\parallel} > T^M_{\perp,\parallel}$ but thermal velocities were taken constant for both cases, i.e. $\theta_{\perp,\parallel} = u_{\perp,\parallel}$.

The aim of present study is to apply the above said methods and investigate the destabilizing effect due to the presence of suprathermal particles on EMEC instability based on kappa-Maxwellian distribution and its comparison with the bi-Maxwellian model. EMEC waves are the right hand circularly polarized waves that were observed first time in the earth's atmosphere as whistlers (Helliwell et al. 1956) and subsequently in many studies such as those triggered by suprathermal electrons and kinetic anisotropies (Mace 1998; Lazar et al. 2008). Since EMEC waves are parallel propagating waves, these are expected to play an important role in solar wind and magnetospheric plasmas. In this manuscript, we employ bi-Maxwellian distribution and two models; Model-I and Model-II for kappa-Maxwellian distribution in order to provide the comparative analysis and to unveil the appropriate model that describes the destabilizing effect of suprathermal plasma particles on EMEC instability.

2 Velocity distributions and models

The bi-Maxwellian function to model anisotropic distribution of velocities is

$$f_M(v_\parallel, v_\perp) = \frac{1}{\pi^{\frac{3}{2}} u_\perp^2 u_\parallel} \exp\left[-\frac{v_\parallel^2}{u_\parallel^2} - \frac{v_\perp^2}{u_\perp^2}\right] \tag{1}$$

where

$$T^M_\parallel = \frac{m u_\parallel^2}{2k_B} \tag{2}$$

$$T^M_\perp = \frac{m u_\perp^2}{2k_B} \tag{3}$$

are the parallel and perpendicular Maxwellian temperatures, respectively. The kappa-Maxwellian distribution, which is the main distribution function under consideration, to model

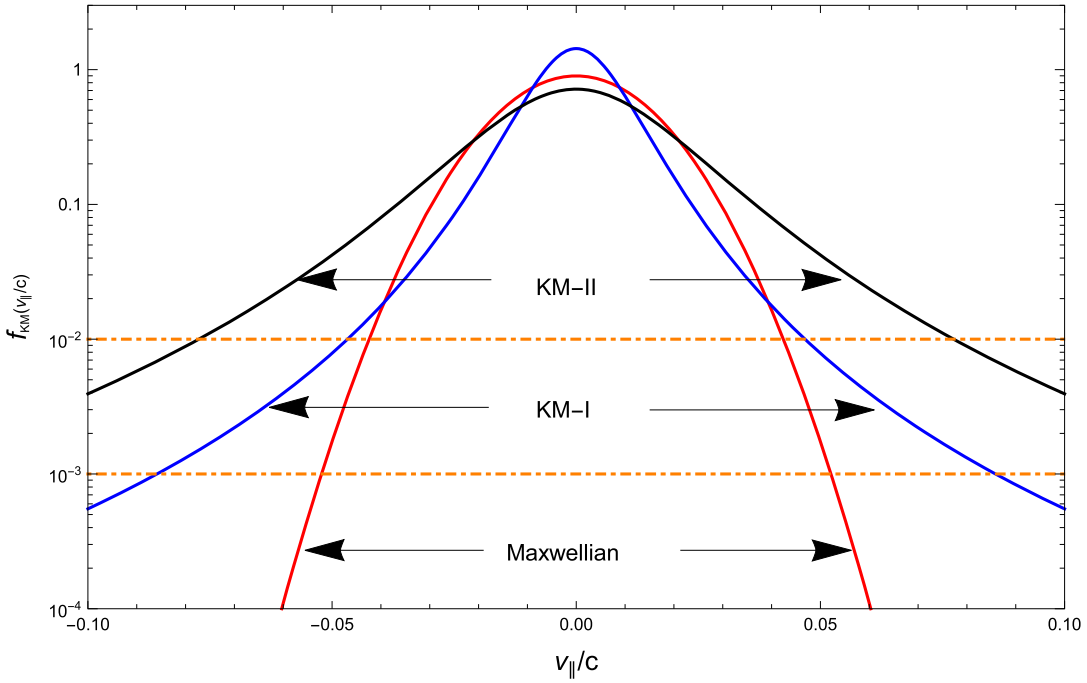

Fig. 1 Parallel cuts of kappa-Maxwellian distributions for case-I (blue), case-II (black) and bi-Maxwellian distribution (red). The dashed-dotted lines represent $f_{KM}(v_\parallel/c) = 10^{-2}$ and $f_{KM}(v_\parallel/c) = 10^{-3}$

anisotropic distribution of velocities is

$$f_{KM}(v_\parallel, v_\perp) = \frac{1}{\pi^{\frac{3}{2}} u_\perp^2 \theta_\parallel} \frac{\Gamma(\kappa+1)}{\kappa^{\frac{3}{2}} \Gamma(\kappa - \frac{1}{2})} \times \left(1 + \frac{v_\parallel^2}{\kappa \theta_\parallel^2}\right)^{-\kappa} \exp\left[-\frac{v_\perp^2}{u_\perp^2}\right] \tag{4}$$

where

$$T_\parallel^{KM} = \frac{m\theta_\parallel^2}{2k_B}\left(\frac{\kappa}{\kappa - 3/2}\right) \tag{5}$$

$$T_\perp^{M} = \frac{m u_\perp^2}{2k_B} \tag{6}$$

are the parallel and perpendicular temperatures, respectively for kappa-Maxwellian distribution, where kappa index should satisfies the condition $\kappa > 3/2$. In the limit $\kappa \to \infty$ kappa-Maxwellian distribution Eq. (4) reduces to the Maxwellian distribution Eq. (1). To investigate the influence of suprathermal population by making a comparison between kappa-Maxwellian and bi-Maxwellian models, we consider the following two models for kappa-Maxwellian distribution.

Model-I: Following Lazar et al. (2015) first we take the temperatures constant, i.e. $T_\parallel^{KM} = T_\parallel^{M}$ and let only parallel thermal velocities different as

$$\theta_\parallel = \sqrt{1 - \frac{3}{2\kappa}}\, u_\parallel \tag{7}$$

since in both models perpendicular motion is characterized by the same manner. Moreover, temperature anisotropy remains constant, i.e. $A^M \equiv \frac{T_\perp^M}{T_\parallel^M} = A^{KM} \equiv \frac{T_\perp^M}{T_\parallel^{KM}}$ which leads to $\frac{T_\perp^M}{T_\parallel^{KM}} = A^M = A$.

Model-II: Alternatively, we consider the thermal velocities to be the same and independent of kappa, i.e. $\theta_{\parallel,\perp} = u_{\parallel,\perp}$ and higher kappa temperature as compared to Maxwellian temperature such as

$$T_\parallel^{KM} = \frac{m\theta_\parallel^2}{2k_B}\left(\frac{2\kappa}{2\kappa - 3}\right) = \frac{2\kappa}{2\kappa - 3} T_\parallel^M > T_\parallel^M \tag{8}$$

Again we take the temperature anisotropy constant, i.e. $A^M \equiv \frac{T_\perp^M}{T_\parallel^M} = A^{KM} \equiv \frac{T_\perp^M}{T_\parallel^{KM}}$ but in this case Eq. (8) leads to $\frac{T_\perp^M}{T_\parallel^{KM}} = A^M(\frac{2\kappa-3}{2\kappa}) = A(\frac{2\kappa-3}{2\kappa})$.

Figure 1 shows the parallel cuts of kappa-Maxwellian distributions for Model-I (blue), Model-II (black) and bi-Maxwellian distribution (red) with $\frac{2u_\perp}{c} = \frac{u_\parallel}{c} = 0.02$. For the Model-I of kappa-Maxwellian distribution we considered $T_\parallel^{KM} = T_\parallel^M$ and thermal velocity $\theta_\parallel$ expressed through Eq. (7). For the Model II we considered $\theta_{\parallel,\perp} = u_{\parallel,\perp}$ and

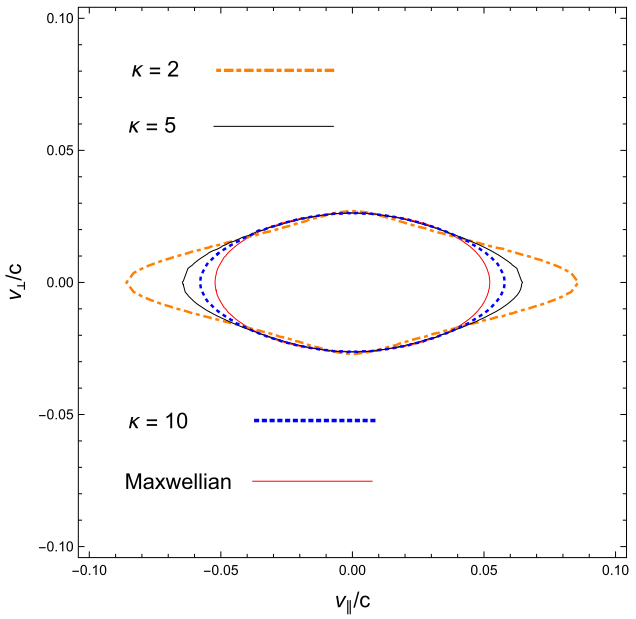

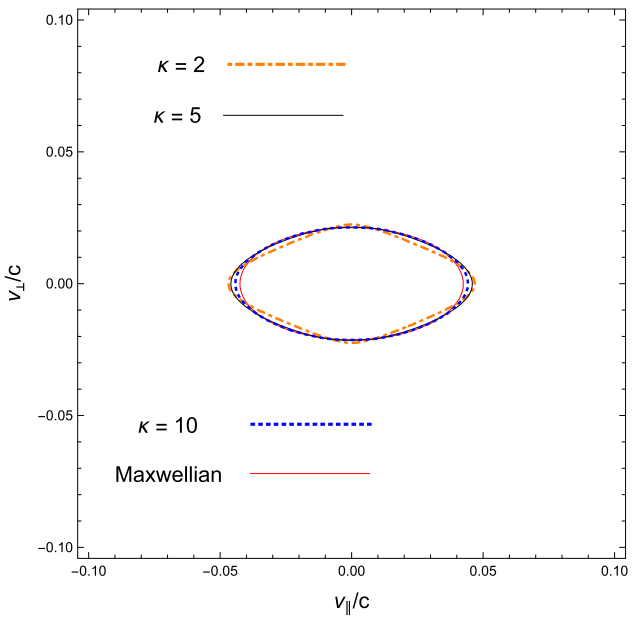

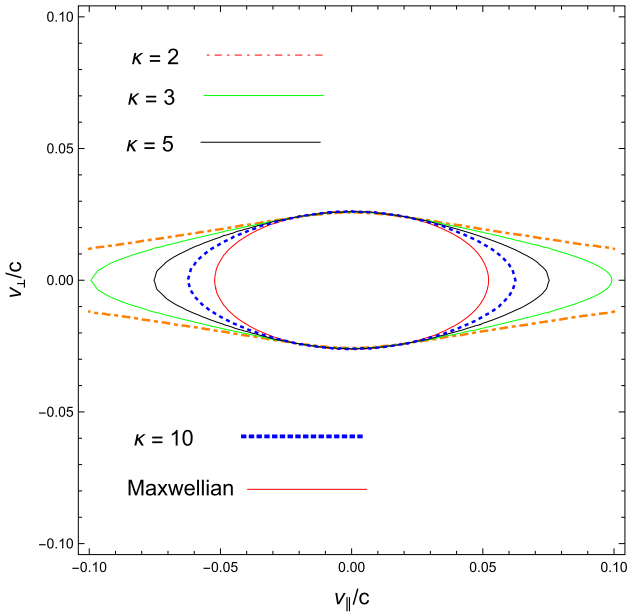

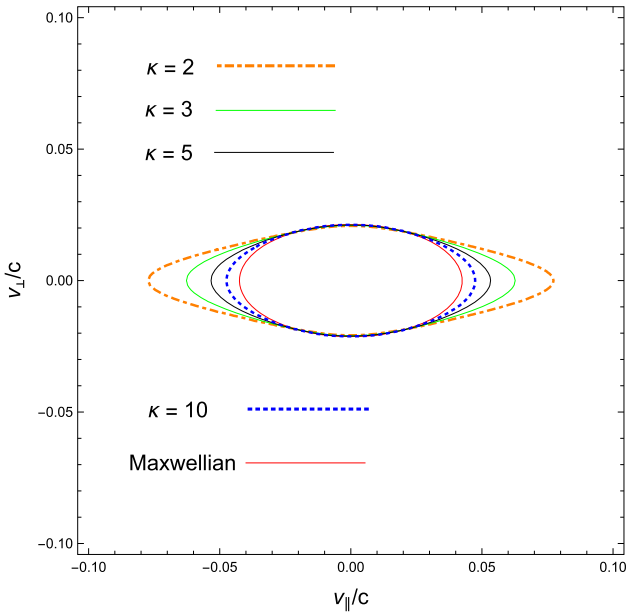

Fig. 2 Contour plots of kappa-Maxwellian distribution for case-I (left panel) and case-II (right panel) for different values of kappa at $f_{KM}(v_\parallel/c) = 10^{-3}$

Fig. 3 Contour plots of kappa-Maxwellian distribution for case-I (left panel) and case-II (right panel) for different values of kappa at $f_{KM}(v_\parallel/c) = 10^{-2}$

$T_\parallel^{KM} > T_\parallel^M$ as given in Eq. (8). Both the models of the kappa-Maxwellian distribution reduce to the bi-Maxwellian distribution in the limit $\kappa \to \infty$..

Figures 2 and 3 show the contour plots of kappa-Maxwellian models for different values of kappa and their limiting bi-Maxwellian model Eq. (1) which can be obtained in the limit $\kappa \to \infty$. Upper panels of Figs. 2 and 3 depict the contours for Model-I of kappa-Maxwellian distribution when $T_\parallel^{KM} = T_\parallel^M$ and $\theta_\parallel$ as given in Eq. (7) at $f_{KM}(v_\parallel/c) = 10^{-3}$ and $f_{KM}(v_\parallel/c) = 10^{-2}$, respectively. The contours are plotted for different values of kappa $\kappa = 2$ (orange), $\kappa = 5$ (black), $\kappa = 10$ (blue) and their limiting Maxwellian form (red) with $\frac{2u_\perp}{c} = \frac{u_\parallel}{c} = 0.02$. Lower panels of Figs. 2 and 3 depict the contours for Model-II of kappa-Maxwellian distribution when $\theta_{\parallel,\perp} = u_{\parallel,\perp}$ and $T_\parallel^{KM} > T_\parallel^M$ as given by Eq. (8) at $f_{KM}(v_\parallel/c) = 10^{-3}$ and $f_{KM}(v_\parallel/c) = 10^{-2}$, respectively. The contours are plotted for different values of kappa $\kappa = 2$ (orange), $\kappa = 3$ (green), $\kappa = 5$ (black), $\kappa = 10$ (blue) and their limiting Maxwellian form (red) with $\frac{2u_\perp}{c} = \frac{u_\parallel}{c} = 0.02$. Comparison of upper and lower panels of Figs. 2 and 3 shows a considerable difference between the anisotropies for the Models-I and II.

The parallel anisotropy for the Model-II is much larger than the anisotropy for the Model-I due to larger parallel kappa-Maxwellian temperature. For both cases, contours tends to become Maxwellian as kappa tends to become infinity.

From Fig. 1, we can note that the Model-II is much hotter and shows a substantial high energy tail as compared to the Model-I, thus possesses excess of free energy. Therefore, Model-II in general could be more realistic case to apply the effect of suprathermal populations in the analysis to investigate their role in the destabilization of waves (Lazar et al. 2015). However, contour plots of kappa-Maxwellian distributions show a large parallel anisotropy for the small values of kappa and secondly the temperature anisotropy $A = \frac{T_\perp^M}{T_\parallel^{KM}}$ reduces due to the presence of factor $(\frac{2\kappa-3}{2\kappa})$, thus could inhibit the growth of EMEC instability for the Model-II kappa-Maxwellian distribution in contrast to the bi-kappa model (Lazar et al. 2015).

3 Dispersion relation of EMEC waves

The general dispersion relation of electromagnetic mode exhibiting right hand circular polarization and propagating along the external magnetic field in spatially homogeneous plasma is

$$\frac{c^2k^2}{\omega^2} = 1 + \frac{\omega_{p\sigma}^2}{2\omega}\int \frac{v_\perp \hat{G} f_\sigma(v_\parallel, v_\perp) d^3\mathrm{v}}{\omega + \Omega_\sigma - kv_\parallel} \tag{9}$$

where $f_\sigma(v_\parallel,\ v_\perp)$ denotes the velocity distribution of plasma species $\sigma = i, e$, $\Omega_\sigma = q_\sigma B_\sigma/(m_\sigma c)$ is the cyclotron frequency, $\omega_{p\sigma} = (\frac{4\pi n_\sigma e^2}{m_\sigma})^{1/2}$ is the plasma frequency for specie of σ kind and

$$\hat{G} = \left(1 - \frac{kv_\parallel}{\omega}\right)\frac{\partial}{\partial v_\perp} + \frac{kv_\perp}{\omega}\frac{\partial}{\partial v_\parallel} \tag{10}$$

is the operator in velocity space. By using distribution function given in Eq. (1) into Eq. (9), we can find that the general dispersion relation for EMEC waves in Maxwellian plasma as

$$\frac{c^2k^2}{\omega^2} = 1 + \frac{\omega_{pe}^2}{\omega^2}\left[-1 + \frac{\Omega_e}{ku_\parallel} Z_M(\xi_M) - \frac{1}{2}\frac{T_\perp^M}{T_\parallel^M} Z'_M(\xi_M)\right] \tag{11}$$

In above equation $Z_M(\xi)$ is the plasma dispersion function (Fried and Conte 1961), given as

$$Z_M(\xi) = \frac{1}{\sqrt{\pi}}\int_{-\infty}^{\infty} \frac{\exp(-s^2)}{(s-\xi)} ds \tag{12}$$

where $\xi_M = \frac{\omega-\Omega}{ku_\parallel}$ and $Z'_M(\xi_M) = -2[1 + \xi_M\ Z_M(\xi_M)]$ is its derivative. Similarly by employing Eq. (4) in Eq. (9), we can get the dispersion relation for EMEC waves in kappa-Maxwellian plasma, as given by

$$\frac{c^2k^2}{\omega^2} = 1 + \frac{\omega_{pe}^2}{\omega^2}\left[-1 + \frac{\Omega_e}{k\theta_\parallel} Z_{\kappa M}(\xi_{KM}) - \frac{1}{2(1-3/2\kappa)}\frac{T_\perp^M}{T_\parallel^{KM}} Z'_{\kappa M}(\xi_{KM})\right] \tag{13}$$

In above equation, $Z_{\kappa M}(\xi_{KM})$ is the modified dispersion function corresponding to kappa-Maxwellian distribution and $Z'_{\kappa M}(\xi_{KM})$ is its derivative which can be expressed in terms of hyper-geometric functions, respectively, as

$$Z_{\kappa M}(\xi_{KM}) = i\frac{(\kappa - 1/2)}{\kappa^{3/2}} {}_2F_1\left[1, 2\kappa; \kappa+1; \frac{1}{2}\left(1 + \frac{i\xi_{KM}}{\sqrt{\kappa}}\right)\right] \tag{14}$$

$$Z'_{\kappa M}(\xi_{KM}) = -\frac{(\kappa - 1/2)}{\kappa(\kappa+1)} {}_2F_1\left[2, 2\kappa+1; \kappa+2; \frac{1}{2}\left(1 + \frac{i\xi_{KM}}{\sqrt{\kappa}}\right)\right] \tag{15}$$

where $\xi_{KM} = \frac{\omega-\Omega}{k\theta_\parallel}$. In deriving the expressions given in Eqs. (11) and (13), we have neglected the ion dynamics and assumed $\Omega_\sigma = \Omega_e$ and $\omega_{p\sigma} = \omega_{pe}$. By considering EMEC waves as subluminal modes, i.e. $\omega^2 \ll c^2\ k^2$ and setting the terms $\frac{T_\perp^M}{T_\parallel^M} = A^M$ and $\frac{T_\perp^M}{T_\parallel^{KM}} = A^{KM}$ the Eqs. (11) and (13) take the form

$$\frac{c^2k^2}{\omega_p^2} = -1 + \frac{\Omega_e}{ku_\parallel} Z_M(\xi_M) - \frac{A^M}{2} Z'_M(\xi_M) \tag{16}$$

$$\frac{c^2k^2}{\omega_p^2} = -1 + \frac{\Omega_e}{k\theta_\parallel} Z_{\kappa M}(\xi_{KM}) - \frac{A^{KM}}{2(1-3/2\kappa)} Z'_{\kappa M}(\xi_{KM}) \tag{17}$$

In the limit $\kappa \to \infty$, Eqs. (13) and (17) reduce to their Maxwellian limits Eqs. (11) and (16), respectively.

4 Numerical solution

In this section, we plot the dispersion relations (16) and (17) numerically to see the effect of suprathermal particles on the growth rate of EMEC instability for a range of plasma beta $0.01 < \beta < 10$ consistent with the observation from terrestrial magnetosphere and solar wind and different values of temperature anisotropy (Stverak et al. 2008). Figure 4 illustrates the variation in normalized real frequency (top panel) and normalized growth rate (bottom panel) of EMEC waves for the Model-I and its Maxwellian limit versus normalized wave numbers for different values of suprathermal index κ

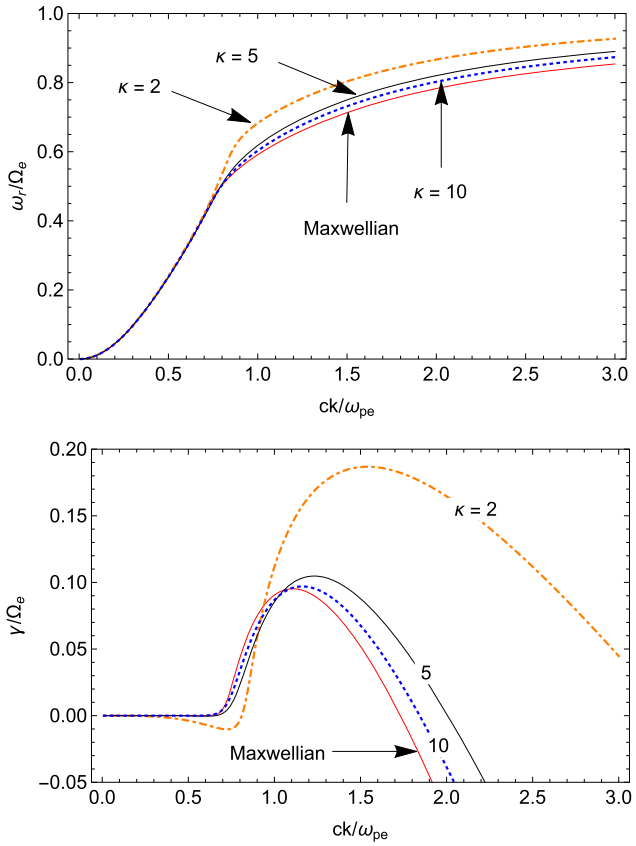

Fig. 4 Dispersion curves of EMEC waves for Model-I with real frequency (top panel) and growth rate (bottom panel) for various values of kappa index when $\beta^M = 0.1$ and $A = 4$

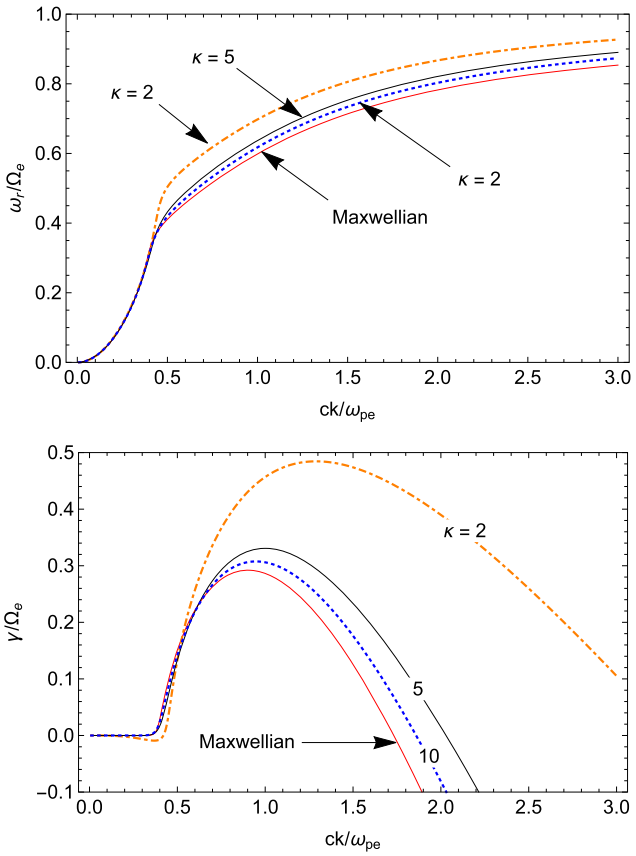

Fig. 5 Dispersion curves of EMEC waves for Model-I with real frequency (top panel) and growth rate (bottom panel) for various values of kappa index when $\beta^M = 0.5$ and $A = 4$

when $\beta^M = 0.1$ and $A = 4$. The growth rate is enhanced as well as the range of unstable wave numbers increases by the presence of suprathermal population as compared to bi-Maxwellian model. Moreover, the minimum and maximum cutoffs of unstable wave numbers shift to their higher values due to the increase of suprathermal particles. The growth rate estimated by kappa-Maxwellian distribution for Model-I first remains slightly lower than the bi-Maxwellian growth rate at smaller wave numbers and then becomes higher than the bi-Maxwellian growth rate as wave number further increases.

Figure 5 depicts the variation in normalized real frequency (top panel) and normalized growth rate (bottom panel) of EMEC waves for the Model-I and its Maxwellian limit versus normalized wave numbers for different values of suprathermal index κ when $\beta^M = 0.5$ and $A = 4$. The general trend is the same as shown in Fig. 4, i.e. growth rate enhances as well as the range of unstable wave numbers increases by the presence of suprathermal population as compared to bi-Maxwellian model, however, growth rate is much higher than the growth rate obtained in Fig. 4. Moreover, minimum cutoff of unstable wave numbers shifts towards the lower wave numbers as compared to in Fig. 4 but maximum cutoff of unstable wave numbers remains the same.

In Fig. 6 the plots of normalized real frequency and normalized growth versus normalized wave numbers are given for Model-II to see the effect of suprathermal particles on EMEC instability when $\beta^M = 0.1$ and $A^M = 4$. Figure 6 reveals that the real frequency is affected non-monotonically by the presence of suprathermal population and shows first decrease and then increase with the increase in normalized wave number. It can also be seen in Fig. 6 that for the Model-II the enhanced suprathermal population causes EMEC wave to damp rather to grow and as suprathermal population decreases wave starts to show growth for $\kappa \geq 3$. Moreover, growth rate for Model-II remains lower than the bi-Maxwellian growth rate and range of unstable wavenumbers remains smaller than the bi-Maxwellian range.

Figure 7 depicts the normalized real frequency and normalized growth rate of EMEC waves versus normalized wave number for Model-II with same temperature anisotropy $A^M = 4$ as in Fig. 4 but for higher value of plasma beta i.e., $\beta^M = 0.5$. Figure 7 shows that growth is obtained even for the lowest value of kappa index, i.e. $\kappa = 2$ but again growth rates for all values of kappa remains lower

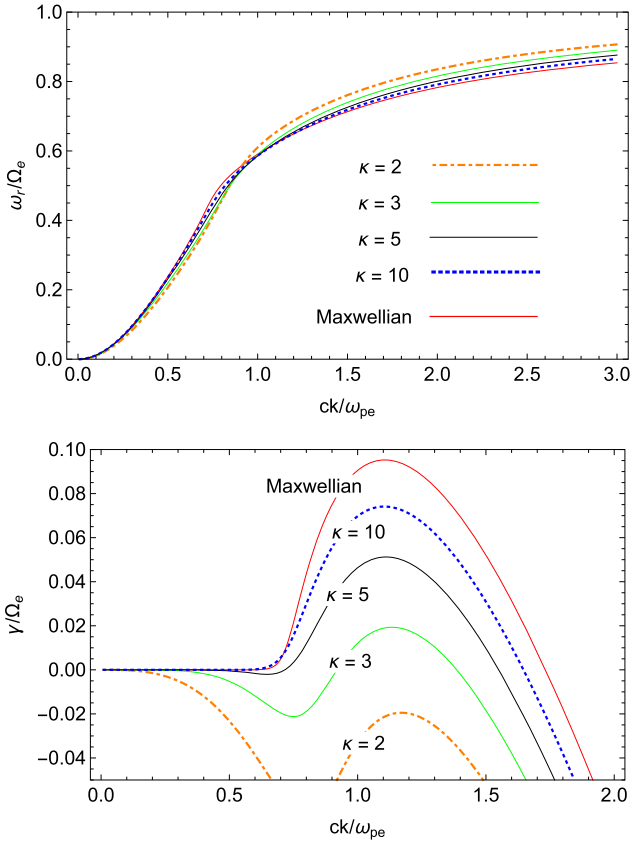

Fig. 6 Dispersion curves of EMEC waves for Model-II with real frequency (top panel) and growth rate (bottom panel) for different values of kappa index when $\beta^M = 0.1$ and $A = 4$

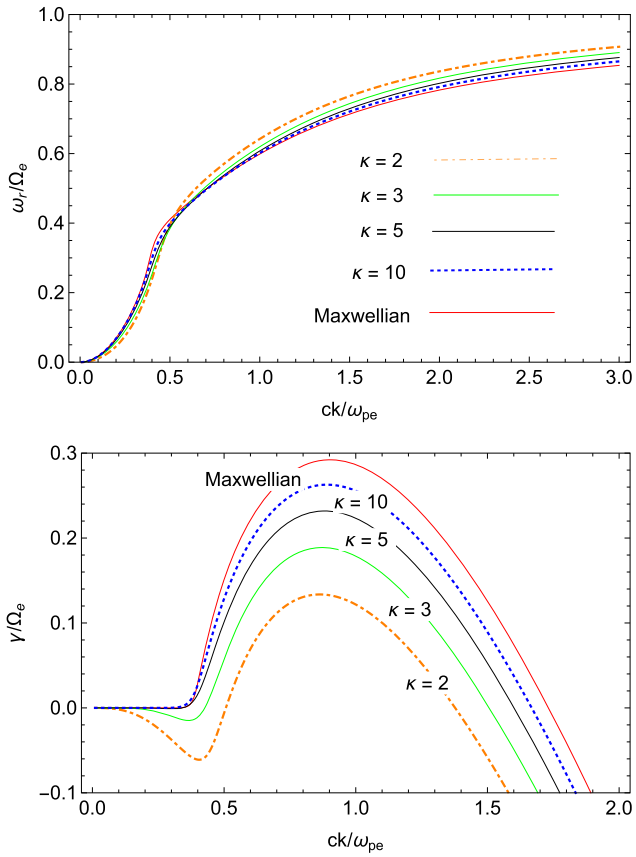

Fig. 7 Dispersion curves of EMEC waves for Model-II with real frequency (top panel) and growth rate (bottom panel) for different values of kappa index when $\beta^M = 0.5$ and $A = 4$

than the bi-Maxwellian growth rate. Growth rate as well as range of unstable wave numbers obtained in Fig. 7 both show enhancement as compared to the corresponding values obtained in Fig. 6. In Fig. 8, we plotted normalized real frequency and normalized growth rate of EMEC waves versus normalized wave number for kappa-Maxwellian Models-I and II for different values of anisotropy $A = 2,\ 3$ when $\beta^M = 2$. We can note that real frequency as well as growth rate increases with the increase in temperature anisotropy for a constant value of plasma beta.

5 Discussion and conclusion

In this paper, we studied EMEC instability by employing kappa-Maxwellian distribution and compare its results with Maxwellian results to unveil the role of suprathermal particles on the destabilization of EMEC instability modelled by kappa-Maxwellian distribution. Earlier studies on EMEC instability in which role of suprathermal particles has been investigated by employing kappa distribution assuming the same effective temperature, resulted in inhibit the instability by enhancing the suprathermal population, i.e. by decreasing the index κ. Since the presence of suprathermal particles indicates the highly nonthermal state of plasma having large amount of free energy which is expected to enhance the kinetic instabilities. This anomaly has been addressed by Lazar et al. (2015) who proposed another variant of kappa model by assuming larger temperature for kappa as compared to Maxwellian but same thermal velocities for both the models. By applying this new variant of kappa distribution, they found the destabilizing effect of EMEC instability with the enhancement in suprathermal particles.

Following Lazar et al. (2015) we proposed two models for kappa-Maxwellian distribution, Model-I and Model-II. In Model-I kappa and Maxwellian temperatures are considered to be the same but thermal velocity for kappa is taken larger than the Maxwellian. We found that EMEC instability based on the kappa-Maxwellian Model-I enhances with the suprathermal population and approaches towards Maxwellian when suprathermal population decreases ($\kappa \to \infty$). In Model-II, temperature for kappa distribution is considered larger than the Maxwellian temperature but thermal velocities for both the distribution are considered to be constant. In contrast to Lazar et al. (2015), the EMEC instability based on the kappa-Maxwellian Model-II inhibits

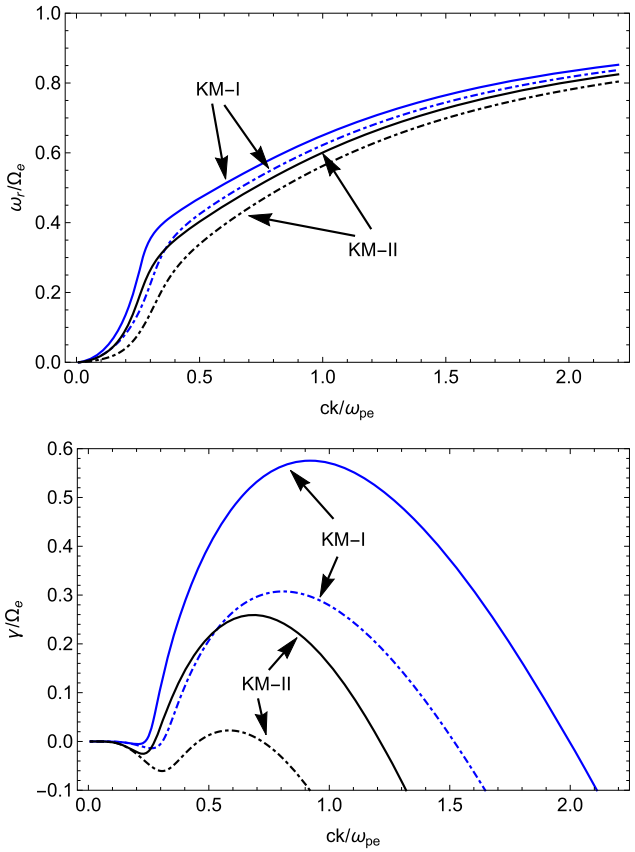

Fig. 8 Dispersion curves of EMEC waves for kappa-Maxwellian Models-I and II with real frequency (top panel) and growth rate (bottom panel) for different values of anisotropy $A = 2$ (dash dotted line) and $A = 3$ (solid line) when $\beta^M = 2$ and $\kappa = 3$

with the suprathermal population and remains lower than the Maxwellian growth rate although Model-II has pronounced high energy tail as compared to Model-I and Maxwellian as shown in Fig. 1. This contrast is due to the nature of the kappa-Maxwellian distribution function such that the resultant anisotropy decreases for Model-II as compared to the Maxwellian anisotropy by a factor of $(\frac{2\kappa-3}{2\kappa})$, i.e. $\frac{T_\perp^M}{T_\parallel^{KM}} = A^M(\frac{2\kappa-3}{2\kappa}) = A(\frac{2\kappa-3}{2\kappa})$, which resulted in inhibiting the growth rate as compared to the Maxwellian growth, and the growth rate decreases with the increase of superthermal populations, i.e. $\kappa \to 3/2$. Figure 8 also depicts this fact that is with the decrease in anisotropy the growth rate reduces. Thus in kappa-Maxwellian plasmas the Model-I truly depicted the role of suprathermal particles in enhancing the EMEC instability in contrast to bi-kappa plasmas.

In conclusion we note that the product kappa-Maxwellian and bi-Kappa distributions are two entirely different distributions and one cannot recover the kappa-Maxwellian from the bi-kappa distribution in the limit $\kappa \to \infty$, but to reduces to a product Maxwellian. Moreover, the same kappa index for parallel and perpendicular directions in bi-kappa distribution where as in kappa-Maxwellian kappa indices for parallel and perpendicular directions are different. Due to these reasons, the anisotropy parameter developed in the dispersions relations for both the models are different. In bi-kappa distribution the anisotropy parameter has parallel and perpendicular temperatures for kappa distribution where as in kappa-Maxwellian case the anisotropy parameter has Maxwellian perpendicular temperature and kappa parallel temperature. This difference in anisotropies causes the opposite results from that of bi-kappa distribution function.

Acknowledgement This research was supported by the GC University grant No.241/ORIC/19 dated 27-08-2019 and National Natural Science Foundation of China Grant No. 41874190.

References

Basu, B.: Phys. Plasmas **15**, 042108 (2008)
Cattaert, T., Hellberg, M.A., Mace, R.L.: Phys. Plasmas **14**, 082111 (2007)
Fried, B.D., Conte, S.D.: The Plasma Dispersion Function. Academic, New York (1961)
Gaelzer, R., Ziebell, L.F., Vinas, A.F., Yoon, P.H., Ryu, C.M.: Astrophys. J. **677**, 676 (2008)
Gary, S.P.: Theory of Space Plasma Microinstabilities. Cambridge University Press, Cambridge (1993)
Hellberg, M.A., Mace, R.L.: Phys. Plasmas **9**, 1495 (2002)
Hellberg, M.A., Mace, R.L., Cattaert, T.: Space Sci. Rev. **121**, 127 (2005)
Helliwell, R., Crary, J., Pope, J., Smith, R.: J. Geophys. Res. **61**, 139 (1956)
Lazar, M.: A & A **547**, A94 (2012)
Lazar, M., Poedts, S.: Astron. Astrophys. **494**, 311 (2009)
Lazar, M., Schlickeiser, R., Poedts, S., Tautz, R.C.: Mon. Not. R. Astron. Soc. **390**, 168 (2008)
Lazar, M., Poedts, S., Schlickeiser, R.: Astron. Astrophys. **534**, A116 (2011)
Lazar, M., Schlickeiser, R., Poedts, S.: Suprathermal particle populations in the solar wind and corona. In: Exploring the Solar Wind (in Tech), ch. 11 (2012). http://www.intechopen.com/books/exploring-the-solar-wind
Lazar, M., Poedts, S., Michno, M.J.: Astron. Astrophys. **554**, A64 (2013)
Lazar, M., Poedts, S., Fichtner, H.: Astron. Astrophys. **582**, A124 (2015)
Mace, R.L.: J. Geophys. Res. **103**, 14643 (1998)
Mace, R.L., Hellberg, M.A.: Phys. Plasmas **10**, 21 (2003)
Mace, R.L., Sydora, R.D., Silin, I.: J. Geophys. Res. **116**, A05206 (2011)
Marsch, E.: Living Rev. Sol. Phys. **3** (2006). http://www.livingreviews.org/lrsp-2006-1
Nazeer, M., Qureshi, M.N.S., Shen, C.: Astrophys. Space Sci. **363**, 160 (2018)
Pierrard, V., Lazar, M.: Sol. Phys. **267**, 153 (2010)
Qureshi, M.N.S., Shah, H.A., Murtaza, G., Schwartz, S.J., Mahmood, F.: Phys. Plasmas **11**, 3819 (2004)
Qureshi, M.N.S., Nasir, W., Masood, W., Yoon, P.H., Shah, H.A., Schwartz, S.J.: J. Geophys. Res. **119**, 10059 (2014)

Qureshi, M.N.S., Nasir, W., Bruno, R.: Mon. Not. R. Astron. Soc. **488**, 954 (2019)
Sehar, Sumbul Qureshi, M.N.S., Shah, H.A.: AIP Adv. **9**, 025315 (2019)
Stverak, S., Travnicek, P., Maksimovic, M., Marsch, E., Fazakerley, A.N., Scime, E.E.: J. Geophys. Res. **113**, A03103 (2008)
Sugiyama, H., Singh, S., Omura, Y., Shoji, M., Nunn, D., Summers, D.: J. Geophys. Res. **120**, 8426 (2015)
Summers, D., Thorne, R.M.: Phys. Fluids B **3**, 1835 (1991)
Treumann, R.A., Baumjohann, W.: Adv. Space Plasma Physics. Imperial College Press, London (1997)
Wu, C.S., Yoon, P.H., Freund, H.P.: Geophys. Res. Lett. **16**, 1461 (1989)
Xue, S., Thorne, R.M., Summers, D.: J. Geophys. Res. **98**, 17475 (1993)
Xue, S., Thorne, R.M., Summers, D.: J. Geophys. Res. **101**, 15467 (1996)